Journal of Applied Ecology

Integrating variation in bacterial-fungal co-occurrence network with soil carbon dynamics

Journal:	*Journal of Applied Ecology*
Manuscript ID	JAPPL-2023-00309.R2
Manuscript Type:	Research Article
Key-words:	Successive planting of Eucalyptus, bacterial-fungal associations, total bacterial diversity, keystone bacterial diversity, soil enzymatic activities, carbon mineralization, SparCC network

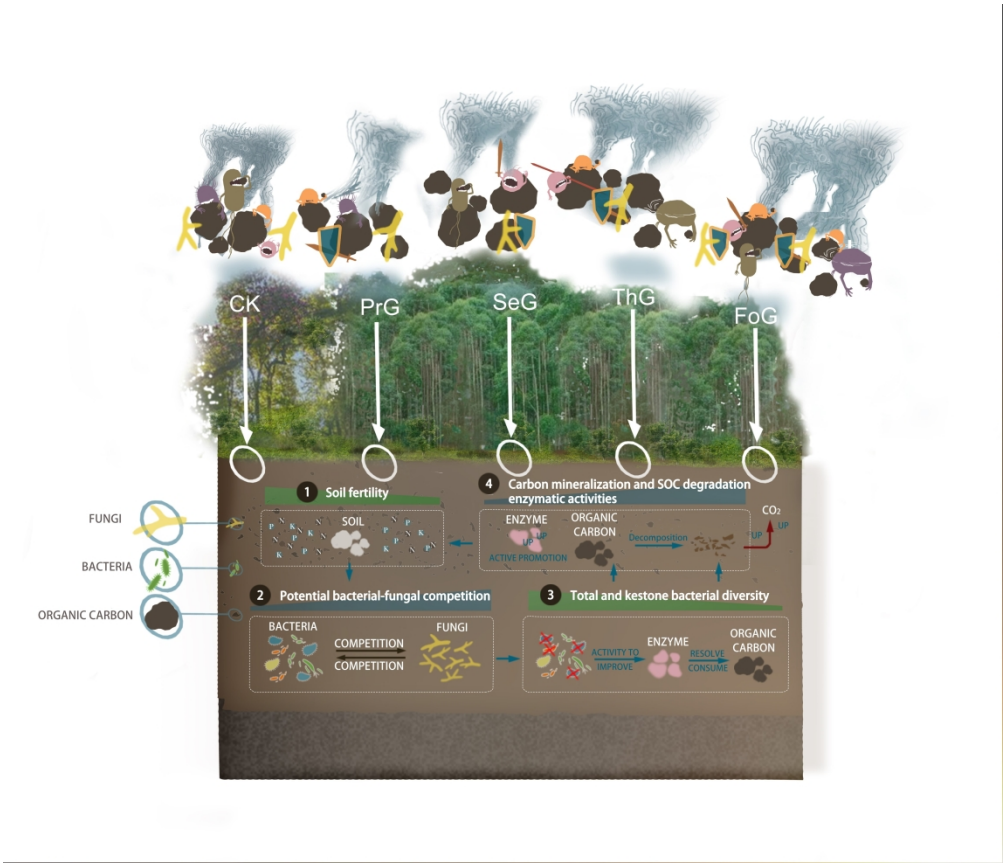

376x323mm (300 x 300 DPI)

1 **Integrating variation in bacterial-fungal co-occurrence network with soil carbon**

2 **dynamics**

Abstract

1. Bacteria and fungi are core microorganisms in diverse ecosystems, and their cross-kingdom interactions are considered key determinants of microbiome structure and ecosystem functioning. However, how bacterial-fungal interactions mediate soil organic carbon (SOC) dynamics remains largely unexplored in the context of artificial forest ecosystems.
2. Here, we characterized soil bacterial and fungal communities in four successive planting of *Eucalyptus* and compared them to a neighboring evergreen broadleaf forest. Carbon (C) mineralization combined with five C-degrading enzymatic activities was investigated to determine the effects of successive planting of *Eucalyptus* on SOC dynamics.
3. Our results indicated that successive planting of *Eucalyptus* significantly altered the diversity and structure of soil bacterial and fungal communities and increased the negative bacterial-fungal associations. The bacterial diversity significantly decreased in all *Eucalyptus* plantations compared to the evergreen forest, while the fungal diversity showed the opposite trend. The ratio of negative bacterial-fungal associations increased with successive planting of *Eucalyptus* due to the decrease in SOC, ammonia nitrogen (NH_4^+−N), nitrate nitrogen (NO_3^-−N), and available phosphorus (AP). Structural equation modeling indicated that the potential cross-kingdom competition, based on the ratio of negative bacterial-fungal correlations, was significantly negatively associated with the diversity of total bacteria and keystone bacteria, thereby increasing C-degrading enzymatic activities and C mineralization.
4. *Synthesis and applications*: Our results highlight the regulatory role of the negative bacterial-fungal association in enhancing the correlation between bacterial diversity and C mineralization. This suggests that promoting short-term successive planting in the

management of *Eucalyptus* plantations can mitigate the impact of this association on SOC decomposition. Taken together, our study advances the understanding of bacterial-fungal negative associations to mediate carbon mineralization in *Eucalyptus* plantations, giving us a new insight into SOC cycling dynamics in artificial forests.

Keywords: Successive planting of *Eucalyptus*; bacterial-fungal associations; total bacterial diversity; keystone bacterial diversity; soil enzymatic activities; carbon mineralization; SparCC network

1 INTRODUCTION

The soil microbiome is a highly diverse ecosystem that is modulated by the dynamic interaction of taxa with and across domains of life (Mould & Hogan, 2021). Microbial interactions have recently received attention for their importance in mediating essential biochemical cycles in soils that directly affect plant performance and productivity (Luo et al., 2019; Fan et al., 2021). Bacteria and fungi have been described to be present in almost all ecosystems, and their spatial proximity can lead to either synergistic or antagonistic interactions (Deveau et al., 2018; Maynard et al., 2019). The bacterial-fungal associations can be modulated by antibiotic metabolism, signaling molecules, protein secretion, and/or organismal modulation of the local physicochemical environment (Velez et al., 2021; Ruan et al., 2022). Ecological bacterial-fungal associations are important for the fitness and colonization rates of interacting partners, ultimately maintaining microbial diversity in various environments (Ghoul & Mitri, 2016; Jiao et al., 2021b). However, the patterns of bacterial-fungal associations that occur naturally in soils remain largely unknown.

Eucalyptus is widely planted in southern China, and most plantations have been established as monocultures with multi-generational successive planting to achieve high timber production (Xu et al., 2020). Long-term monoculture has caused numerous ecological problems, such as soil degradation and loss of soil microbial diversity and ecosystem stability (Xu et al., 2021). Previous studies have reported strong negative associations between the saprotrophic fungal and bacterial community in *Eucalyptus* plantations (Chen et al., 2021). The changes in community diversity and bacterial-fungal associations may largely depend on successive generations, as high generations of *Eucalyptus* plantations substantially reduce soil fertility by reducing the inputs of litter and root exudate (Ismaw et al., 2012; Veldkamp et al., 2020). Keystone taxa are considered

key components of microbial communities that regulate diversity and community functions through high potential interactions (Trivedi et al., 2020). The presence of keystone species has profound effects on the nature and magnitude of bacterial-fungal associations (Herren & McMahon, 2018; Chen et al., 2019). Whether and to what extent successive planting of *Eucalyptus* regulate microbial diversity and bacterial-fungal associations is an unanswered question that has been overlooked in current management practices for years.

Soil organic carbon (SOC) is defined as the core property of soil, and SOC formation and mineralization are central to climate regulation, food production, habitat conservation, and nutrient cycling (Lehmann & Kleber, 2015). Understanding and quantifying the response of SOC to bacterial-fungal associations is essential for regulating SOC dynamics (Mille-Lindblom & Tranvik, 2003; Sokol et al., 2022). Bacterial-fungal cooperation is an important pathway for SOC mineralization, and functional complementarity between these two groups may influence soil carbon metabolic capacity (van der Heijden et al., 2016; Durán et al., 2018). However, bacteria and fungi are known to share simple plant-derived substances (e.g., amino acids and sugars), and antagonistic bacterial-fungal associations induced by substrate competition can enhance carbon consumption and decomposition (de Boer et al., 2005; Cecilia et al., 2006). Microbial species in highly competitive communities often grow with low carbon efficiency due to the high energy invested in competition, suggesting that the strongly antagonistic interactions can cause high C resource consumption (Becker et al., 2012; Maynard et al., 2017a). Keystone taxa have great explanatory power for community function, and changes in keystone taxa diversity considerably influence the strength and direction of SOC dynamics (Berry & Widder, 2014; Fan et al., 2021). Bacterial-fungal co-occurrence patterns have long been of interest to microbial ecologists, but

76 little attention has been paid to their impact on the microbial diversity-function relationships that
77 underlie SOC dynamics.

78 *Eucalyptus* has valuable economic importance in maintaining the world's timber supply
79 (Hunter, 2001). Most *Eucalyptus* plantations in southern China are short-rotation (4–6 years), and
80 successive planting of *Eucalyptus* can cause soil degradation with nutrient losses of nitrogen,
81 phosphorus, and potassium (Temesgen et al., 2016; Zhu et al., 2019). In the present study, we
82 sought to assess the structure of soil bacterial and fungal communities and patterns of bacterial-
83 fungal co-occurrence potentially associated with SOC dynamics in response to successive
84 planting of *Eucalyptus*. Specifically, this study focused on testing three hypotheses: (*i*) the
85 successive planting of *Eucalyptus* will significantly affect the diversity and taxa co-occurrence
86 patterns of bacterial and fungal communities; (*ii*) the negative bacterial-fungal associations will
87 decrease bacterial diversity in the successive planting of *Eucalyptus*, as well as the diversity of
88 keystone taxa; and (*iii*) the diversity and negative co-occurrence pattern of bacterial and fungal
89 communities will jointly improve SOC mineralization.
90

91 **2 MATERIALS AND METHODS**

92 **Experimental site description**

93 The experimental site is located in the state-owned Daguishan Forest Farm in Hezhou City,
94 Guangxi Zhuang Autonomous Region, China (111°20'5''E, 23°58'33''N). The mean annual
95 temperature in this area is 19.3℃, with mean annual precipitation and evaporation of 2,056 mm
96 and 1,200 mm, respectively. The soil type is classified as red soil (i.e., ferralsols). A total of 12
97 plots (20 m wide × 30 m long) were established to collect soil samples in triplicate representing

four generations of *Eucalyptus* plantation. In each treatment, the *Eucalyptus* trees were at the same stage of development (i.e., 4 years after planting). The treatments included the first generation (PrG) of *Eucalyptus* reforestation, the second generation (SeG) regenerating after the PrG was cut, the third generation (ThG) regenerating after the SeG, and the fourth generation (FoG) regenerating after the ThG. An evergreen broadleaf forest with three adjacent plots was selected as the control (CK), which was a precursor to the *Eucalyptus* plantation. All the plots were located within a 5 km^2 area. The *Eucalyptus* species planted in these plots was a hybrid of *Eucalyptus urophylla S.T. Blake* × *Eucalyptus grandis Hill ex Maiden* (*Eucalyptus urograndis*).

Soil sampling, physiochemical analysis, and microbial biomass

Fifteen soil cores were collected from each plot using the "S" line soil sampling strategy and then mixed evenly as a composite sample. Soil samples were collected from 15 plots (5 treatments × 3 replicates) at a depth of 0−20 cm in July 2020. Samples were collected in sterile plastic bags and immediately transported to the laboratory (<12 h). After sieving (< 4 mm), each sample was divided for determination of soil chemical properties, the bacterial and fungal communities, soil enzymatic activities and carbon mineralization.

Soil bulk density was determined using 43 cm^3 standard cylinders and by calculating total porosity (Pt) and aeration porosity (Pa). Soil pH was determined using a glass electrode pH meter (Sartorius, Germany) with a soil:water ratio of 1:2.5. Soil organic carbon (SOC) and total nitrogen (TN) were determined using the $K_2Cr_2O_7$-H_2SO_4 oxidation method and the semi-micro Kjeldahl method, respectively. Soil ammonium nitrogen (NH^{4+}−N) and nitrate nitrogen (NO_3^-−N) concentrations were measured using a flow analyzer (Astoria-Pacific 2-channel flow analyzer).

120 Total phosphorus (TP) and available phosphorus (AP) were determined by MoSb colorimetry,
121 and total potassium (TK) and available potassium (AK) were determined by flame
122 spectrophotometry. Soil cation exchange capacity (CEC) was determined using ammonium
123 acetate solution at pH = 7 (Sparks & Page, 1996). Soil microbial biomass carbon, nitrogen and
124 phosphorus (i.e. MBC, MBN and MBP) were measured by the chloroform fumigation method
125 (Jenkinson & Powlson, 1976).
126
127 **Soil enzymatic activities and cumulative carbon mineralization**
128 Five C-degrading enzymatic activities were determined, including β-1,4-glucosidase (BG, EC
129 3.2.1.21), sucrase (EC 3.2.1.26), β-xylosidase (BX, EC 3.2.1.37), β-N-acetylglucosaminidase
130 (NAG, EC 3.1.6.1), and acid phosphatase (ACP, EC 3.1.3.2) (Manju & Chadha, 2011; Chen et
131 al., 2018; Lustenhouwer et al., 2020). The activities of these hydrolytic enzymes were determined
132 using the 4-methylumbelliferyl (MUB), which produces the highly fluorescent cleavage products
133 MUB upon substrate hydrolysis. Assays were performed in 96-well microplates as described by
134 Bell et al (2013). Six replicates of each sample were set up, and each standard concentration
135 shared the same number of replicates. Assay plates were incubated in the dark at 25°C for 3 h,
136 and enzymatic activities in each plate were corrected using a quench control. A microplate
137 fluorometer (EnSpire 2300 Multilabel Reader, Perkin Elmer, Waltham, MA, USA) was used to
138 measure fluorescence using the 365 nm excitation and 460 nm emission filters. The enzymatic
139 activities were expressed as μmol g^{-1} dry soil h^{-1}.
140 Soil C mineralization potential was determined by microcosm incubation according to Ribeiro
141 et al. (2010). Briefly, a subset of air-dried soil samples (i.e., 20 g per sample) were adjusted and

maintained (using distilled water) at a moisture content of 60% of field capacity and incubated in 500 mL sealed vessels with rubber septa at 25℃ for 72 days. Each vessel was placed in a small beaker containing 10 ml of 0.5 mol l^{-1} NaOH solution to completely absorb CO_2 emissions from the soil samples. After incubation for 1, 3, 5, 7, 10, 18, 26, 34, 42, 50, and 72 d, the beaker in each vessel was carefully removed and replaced with 0.1 mol l^{-1} HCl solution to titrate the remaining NaOH. After each sampling, the jars were opened for 1 h to allow air exchange to restore normal oxygen levels. Three jars without soil sample were collected simultaneously and served as background controls. Potential C mineralization was calculated from the cumulative amount of C produced per unit of soil (i.e., mg CO_2-C per kg soil).

DNA extraction and high-throughput sequencing

Total DNA was extracted from 0.5 g soil samples using the MoBio PowerSoil DNA extraction kit (Carlsbad, CA, USA) following the manufacturer's protocol. DNA concentration and quality were determined using a NanoDrop ND-1000 spectrophotometer (NanoDrop Technologies, Wilmington, DE, USA). Illumina sequencing data of the bacterial 16S rRNA gene and the fungal ITS region were used to determine the diversity, composition, and network structure of the soil bacterial and fungal communities. The bacterial 16S rRNA gene and the fungal ITS region were sequenced using the primer sets 338F/806R (Lee et al., 2012) and ITS1-1737F/ITS2-2043R (Bazzicalupo et al., 2013), respectively. Quantitative Insights into Microbial Ecology (QIIME, version 1.9.1) software was used for quality screening and trimming of the raw sequence data (Caporaso et al., 2010). Filtered reads were subjected to *de novo* chimera detection in UCHIME (Edgar et al., 2011), and frame shifts using HMM-FRAME (Zhang et al., 2011). Community-

164 level analysis for the 16S rRNA gene and the fungal ITS region was based on operational
165 taxonomic units (OTUs) with 97% nucleotide identity (He et al., 2015). Taxonomy was assigned
166 to bacteria and fungi using the Basic Local Alignment Search Tool (BLAST) for each
167 representative sequence against the Silva Release 128 and UNITE version 6.0 databases,
168 respectively (Quast et al., 2013; Kõljalg et al., 2013). Alpha diversity and beta diversity (based
169 on Bray-Curtis distances) of soil bacterial and fungal communities were calculated after rarefying
170 to 26,074 and 58,017 sequences per sample, respectively.
171
172 **Statistical analyses**
173 One-way analysis of variance (ANOVA) was used to test for differences in soil properties,
174 microbial biomass, fungal and bacterial diversity, enzymatic activity, and C mineralization rates
175 using the Bonferroni's post hoc test in SPSS 20.0 (SPSS, Chicago, IL, USA). Metrics of bacterial
176 and fungal alpha diversity (i.e., Shannon index and Chao1 richness) and principal coordinate
177 analysis (PCoA) were calculated using the 'vegan' package in R (R 4.0.3, R Development Core
178 Team). The multiple regression model (lm function in 'stats' package) and variance
179 decomposition analysis (calc. relimp function in the 'relaimpo' package) were used to estimate
180 the importance of soil physicochemical properties in explaining variation in fungal and bacterial
181 diversity and differences in microbial biomass (Grömping, 2006). Permutational multivariate
182 analysis of variance (PERMANOVA) based on Bray-Curtis dissimilarity was used to examine
183 differences between treatments.
184 We constructed bacterial-fungal co-occurrence networks using SparCC with the iNAP
185 network analysis pipeline (Feng et al., 2022). Only OTUs with ≥12 occurrences (from a total of

186 15 samples) were retained for network analysis. The co-occurrence of OTUs was determined with
187 parameters of $r > 0.7$ or $r < -0.7$ and $P < 0.05$ (Friedman & Alm, 2012). The P values below 0.05
188 were subjected to a test correction using the Benjamini-Hochberg procedure to prevent false
189 correlations. We extracted subnetworks by preserving the OTUs (including edges between these
190 OTUs) present in individual soil samples using the 'induced_subgraph' function in the 'igraph'
191 package (Ma et al., 2015; Jiao et al., 2021a). Significant co-occurrences were plotted and
192 visualized using Gephi (0.9.1) (Bastian et al., 2009). Nodes indicate individual OTUs, and edges
193 represent the pairwise associations between nodes. Network modules were clusters of closely
194 related nodes obtained using the molecular complex detection based on the Cytoscape platform
195 (Bader et al., 2003). We identified two topological parameters: the within-module connectivity Z_i
196 and the among-module connectivity P_i. All nodes were classified as network hubs ($Z_i > 0.25$, $P_i >$
197 0.62), module hubs ($Z_i > 0.25$, $P_i \leq 0.62$), connectors ($Z_i \leq 0.25$, $P_i > 0.62$), or peripherals ($Z_i \leq$
198 0.25, $P_i \leq 0.62$) (Olesen et al., 2007). Consequently, nodes with either a high value of Z or P were
199 defined as potential keystone taxa, including network hubs, module hubs, and connectors.

200 Random forest modeling was used to quantitatively evaluate the relative importance of soil
201 abiotic and biotic properties on carbon mineralization. Soil abiotic properties included soil pH,
202 TN, TP, TK, NO_3^-–N, NH_4^+–N, AP, AK, CEC, bulk density, Pt, and Pa, while biotic properties
203 included the biomass, diversity, and composition of bacterial and fungal communities, bacterial-
204 fungal network, and enzymatic activities. Microbial biomass was characterized by MBC, MBN
205 and MBP. The Shannon index and Chao1 richness were used for bacterial and fungal diversity.
206 The first principal coordinate (PCoA1) was used as a parameter to explain the variations in soil
207 bacterial and fungal communities. The hydrolytic enzymes β-1,4-glucosidase, β-xylosidase, acid

208 phosphatase, sucrase and β-N-acetylglucosaminidase were used as enzymatic activities. The
209 bacterial-fungal network was used to extract the number of negative:positive associations of
210 bacterial-bacterial, fungal-fungal, and bacterial-fungal OTUs. Structural equation modeling
211 (SEM) was performed to examine the influence of soil properties and microbial community
212 structure on C mineralization and SOC dynamics. Based on the random forest analyses, the
213 significant ($P < 0.05$) predictors were further selected to perform structural equation modeling
214 (SEM) analysis. SEM analysis was conducted using the robust partial least squares evaluation
215 method with AMOS 20.0 (AMOS IBM, USA). SEM fitness was assessed based on a non-
216 significant chi-square test ($P > 0.05$), the goodness-of-fit index, and the root mean square error of
217 approximation (Byrne, 2010).
218

219 **3 RESULTS**

220 **Soil properties, enzymatic activities, and carbon mineralization**

221 Successive planting of *Eucalyptus* significantly affected soil physicochemical properties ($F_{(4, 10)}$ =
222 3.54~291.89, $P < 0.05$). Soil pH, soil organic carbon (SOC), total nitrogen (TN), total phosphorus
223 (TP), ammonium nitrogen (NH_4^+−N), and available potassium (AK) were significantly ($P < 0.05$)
224 lower in *Eucalyptus* plantations (PrG, SeG, ThG and FoG treatments) compared to the control
225 treatment (CK) of the evergreen forest. However, these soil properties also tended to decrease
226 with successive planting of *Eucalyptus* (**Fig. 1a, Table 1**). Nitrate nitrogen (NO_3^-−N), total
227 potassium (TK) and available phosphorus (AP) also significantly decreased ($P < 0.05$) over the
228 years of *Eucalyptus* planting. Cation exchange capacity (CEC) ranged from 15.92 to 21.77 cmol
229 kg^{-1}, with a significantly higher value ($P < 0.05$) in PrG and SeG treatments compared to CK

230 treatment. No significant differences were found for bulk density, total porosity, and aeration
231 porosity among the *Eucalyptus* planting treatments (**Table 1**).

232 Carbon mineralization was significantly lower ($P < 0.05$) in PrG and SeG treatments than in
233 CK, ThG, and FoG treatments (**Fig. 1b**). Compared with CK treatment, *Eucalyptus* planting
234 significantly ($P < 0.05$) decreased the enzymatic activities of sucrase (33.3%~64.0%), β-1,4-
235 glucosidase (BG, 15.7%~38.9%), β-xylosidase (BX, 52.2%~63.2%), acid phosphatase (ACP,
236 58.7%~71.7%), and β-N-acetylglucosaminidase (NAG, 51.0%~76.3%) (**Fig. 1c**). BG and ACP
237 activities were significantly ($P < 0.05$) higher in SeG, ThG, and FoG treatments than in PrG
238 treatment. Sucrase activity was significantly ($P < 0.05$) lower in PrG, ThG, and FoG treatments
239 than in CK and SeG treatments. However, BX and NAG activities were not significantly ($P >$
240 0.05) different among the *Eucalyptus* planting treatments (**Fig. 1c**).

241

242 **Microbial biomass and diversity**

243 Microbial biomass measured as MBC, MBN and MBP significantly ($P < 0.05$) varied among the
244 *Eucalyptus* planting treatments. The ThG and FoG treatments significantly ($P < 0.05$) decreased
245 MBC by 40.8% and 49.0%, MBN by 93.1% and 95.1%, and MBP by 88.5% and 89.4% compared
246 to CK and SeG treatments, respectively (**Fig. S1**). The Shannon index of bacterial communities
247 significantly ($P < 0.05$) decreased with increasing years of *Eucalyptus* plantation. However, the
248 Shannon index and Chao1 richness of fungal communities showed an opposite pattern (**Fig. 2a,**
249 **b**). The Shannon index and Chao1 richness of bacterial communities were significantly ($P < 0.05$)
250 higher in SeG treatment than in FoG treatment, while these indices for fungal communities were
251 significantly ($P < 0.05$) higher in ThG treatment than in SeG and PrG treatments.

252 The multiple regression model combined with variance decomposition analysis revealed that
253 AP, NH_4^+−N, NO_3^-−N, and SOC were strong predictors of changes in microbial biomass (7.0%
254 to 19.3%, $P < 0.05$), followed by bacterial and fungal Shannon index (5.6% to 8.8% and 6.8% to
255 16.8%, $P < 0.05$) (**Fig. 2c**). AP, NH_4^+−N, NO_3^-−N, and SOC were positively correlated with
256 bacterial Shannon index ($r = 0.54$ to 0.81, $P < 0.05$), MBC ($r = 0.68$ to 0.93, $P < 0.01$), MBN (r
257 = 0.51 to 0.91, $P < 0.05$) and MBP ($r = 0.57$ to 0.86, $P < 0.05$), and negatively correlated with the
258 fungal Shannon index ($r = -0.58$ to -0.67, $P < 0.05$) (**Fig. 2c**).
259
260 **Taxonomic composition of soil bacterial and fungal communities**
261 The soil bacterial communities were mainly composed of the phyla Proteobacteria (43.1%),
262 Acidobacteria (33.2%), Actinobacteria (7.90%), Chloroflexi (7.20%), Verrucomicrobia (2.60%),
263 and Firmicutes (2.19%) (**Fig. S2a**). At the genus level, the bacterial community was dominated
264 by DA111 (13.8%), *Edaphobacter* (10.0%), *Variibacter* (5.82%), *Acidothermus* (4.98%),
265 *Candidatus_Solibacter* (4.77%), *Bradyrhizobium* (3.44%), *Acidibacter* (3.90%), *Rhodanobacter*
266 (2.30%), and *Bryobacter* (2.02%) (**Fig. S2c**). The fungal community consisted of the dominant
267 phyla Ascomycota (63.1%), Basidiomycota (18.3%), and Zygomycota (17.1%), followed by the
268 rare phyla Glomeromycota (0.55%) and Chytridiomycota (0.22%) (**Fig. S2b**). At the genus level,
269 the fungal community was dominated by *Umbelopsis* (9.40%), *Penicillium* (4.79%), *Russula*
270 (3.47%), *Tetracladium* (1.65%), *Issatchenkia* (0.98%), and *Scleroderma* (0.91%) (**Fig. S2d**).
271 Principal coordinate analysis (PCoA) combined with permutational multivariate analysis of
272 variance indicated that the composition of the bacterial community in PrG, SeG, and ThG
273 treatments was significantly ($P = 0.001$) different from those in FoG and CK treatments (**Fig.**

274 **S3a**). The relative abundance of Proteobacteria and Actinobacteria was higher in PrG, SeG, and
275 ThG treatments, while that of Acidobacteria was higher in CK and FoG treatments (**Fig. S3a**, P
276 < 0.05). Similar to the bacterial communities, PCoA revealed that the differences in the
277 composition of the fungal communities by *Eucalyptus* planting treatments were also significantly
278 (P = 0.001) different from CK treatment. The four *Eucalyptus* treatments had significantly (P <
279 0.05) higher relative abundances of Zygomycota and Ascomycota, and lower relative abundances
280 of Basidiomycota compared to CK treatment (**Fig. S3b**). Mantel test indicated that the structure
281 of bacterial and fungal communities was significantly associated with variations in soil pH, SOC,
282 NH_4^+−N, TN, TP, and AP (r = 0.27~0.42, P < 0.01), and thus indirectly associated with variations
283 in soil microbiome structure mediated by successive *Eucalyptus* planting (**Fig. S3c**).
284
285 **Microbial co-occurrence networks**
286 The network analysis resulted in a network with 998 nodes and 6402 edges, a diameter of 5, an
287 average degree of 6.415, an average path length of 3.796, a modularity of 0.543, and an average
288 clustering coefficient of 0.169. The bacterial and fungal taxa contributed 57.9% and 42.1% of the
289 nodes, respectively (**Fig. 3a-c**). Correlations between bacterial OTUs accounted for 41.7%,
290 between fungal OTUs for 27.3%, and between bacterial and fungal OTUs for 31.0%. The
291 bacterial-bacterial and fungal-fungal associations were mainly positive (40.0% and 22.4% of total
292 edges), whereas the bacterial-fungal associations were primarily negative (24.9%) (Fig. 3d) (**Fig.**
293 **3d**). We found that there was a general trend to increase the number of negative bacterial-fungal
294 correlations (26.6% and 25.4%, respectively) through the *Eucalyptus* planting generations (ThG
295 and FoG treatments), as indicated by the ratios of negative edges to positive edges (**Fig. 3e**).

296 Based on the network topological metrics, two bacterial OTUs belonging to the family
297 Caulobacteraceae (phylum Proteobacteria) and Xiphinematobacteraceae (phylum
298 Verrucomicrobia) were identified as network hubs (**Fig. 4a, Table S1**). A total of 21 and 134
299 nodes were identified as module hubs (13 bacterial and 7 fungal taxa) and connectors (75 bacterial
300 and 59 fungal taxa). The potential bacterial keystone taxa were mostly affiliated with
301 Proteobacteria, Acidobacteria, Chloroflexi, and Verrucomicrobia, while the potential fungal
302 keystone taxa were primarily affiliated with Ascomycota, Basidiomycota, and Zygomycota (**Fig.**
303 **4a, Table S1**). The Shannon index of bacterial keystone taxa was significantly ($P < 0.05$) higher
304 in four *Eucalyptus* plantations than in CK treatment (**Fig. 4b**). Moreover, this index was
305 significantly ($P < 0.05$) higher in SeG treatment than in ThG and FoG treatments. However, there
306 was no significant ($P > 0.05$) difference in the Shannon index and Chao1 richness of fungal
307 keystone taxa, except that the Chao1 richness was significantly higher in ThG treatment than in
308 PrG treatment (**Fig. 4b**).
309
310 **Negative bacterial-fungal associations correlated with carbon mineralization**
311 Random forest modeling showed that all predictors significantly contributed to carbon
312 mineralization (67.9%, $P < 0.05$) (**Fig. S4**). Soil pH, TN, and NH_4^+−N were the stronger
313 determinants of carbon mineralization (2.1%~6.9%, $P < 0.05$). To a lesser extent, carbon
314 mineralization was significantly ($P < 0.05$) predicted by Shannon index of total bacteria (4.2%)
315 and keystone bacteria (2.8%), fungal-bacterial correlations (3.2%), and soil enzymatic activities
316 (BG, BX, and Sucrase) (4.4%~4.7%) (**Fig. S4**). Structural equation modeling provided further
317 statistical evidence that keystone bacterial diversity was positively correlated with soil properties

318 (r = 0.759, P < 0.001) and total bacterial diversity (r = 0.742, P < 0.01). The negative bacterial-
319 fungal associations were negatively correlated with total bacterial diversity (r = −0.688, P < 0.01).
320 Furthermore, the diversity of total bacteria (through BX, r = −0.649, P < 0.05) and keystone
321 bacteria (through BG, r = −0.404, P < 0.05 and sucrase, r = 0.339, P < 0.05) were negatively
322 correlated with C-degrading enzymatic activities and C mineralization (**Fig. 5a**). Consistent with
323 the result of random forest modeling, SEM indicated that general patterns of bacterial-fungal
324 negative associations, the diversity of total bacteria and keystone bacteria may have strong effects
325 on C- degrading enzymatic activities and C mineralization (**Fig. 5b, c**).
326

327 **4 DISCUSSION**

328 **Successive planting of *Eucalyptus* affected the bacterial and fungal communities**
329 We observed that successive planting of *Eucalyptus* significantly decreased the bacterial diversity,
330 but improved the fungal diversity due to changes in SOC, NH_4^+−N, NO_3^-−N, and AP (**Table 1**).
331 Soil organic carbon is widely recognized as a key regulator influencing microbial diversity (Zhang
332 et al., 2020). Continuous tree harvesting in *Eucalyptus* plantations significantly decreases SOC
333 by reducing litter and root exudate inputs (Guillaume et al., 2015; Chen et al., 2021). *Eucalyptus*
334 residues contain high amounts of recalcitrant organic biopolymers, and the accumulation of
335 recalcitrant compounds in the soil after successive plantings may favor more fungal species and
336 suppress bacterial growth (Mori et al., 2020). In general, soil fungi have a high ability to acquire
337 resources, which allows them to be more adaptable to low SOC environments, and thus the
338 decrease in SOC has less or even positive effects on fungal diversity (Yang et al., 2019). In
339 contrast, bacteria may preferentially use labile organic compounds and grow with low C

efficiency, and the degradation of SOC quantity and quality caused by successive planting of *Eucalyptus* reduced bacterial diversity. The relative abundance of *Acidibater* and *Candidatus-Solibacte* decreased in the third and fourth planting generations, which was partly responsible for the decrease in bacterial diversity. *Acidibater* and *Candidatus-Solibacte* prefer carbohydrates (e.g., hexoses, amino acids, lactose, and galactose) as their main carbon source (Pearce et al., 2012; Falagán et al., 2014), and low concentrations of liable carbon ultimately reduce the growth rates of these genera (Xu et al., 2021). In addition, the successive planting of *Eucalyptus* reduced NH_4^+−N, NO_3^-−N, and AP by two to three times compared to CK treatment. Considering that nutrient availability was a limiting factor for bacterial and fungal growth, microbial biomass (as indicated by MBC, MBN, and MBP) and diversity significantly decreased with successive planting of *Eucalyptus*, especially after two generations. The bacterial community is widely known to be less adapted to oligotrophic environments than the fungal community, and thus the decrease in NH_4^+−N, NO_3^-−N, and AP directly reduces bacterial biomass and diversity by inhibiting growth and cell proliferation (de Vries et al., 2018; Zhu et al., 2019).

Negative bacterial-fungal associations decreased bacterial diversity

Our study showed that the negative bacterial-fungal associations increased with increasing generations of *Eucalyptus*, indicating the long-term *Eucalyptus* planting dominated the potential negative interactions between fungi and bacteria. The negative bacterial-fungal associations may be due to interference confrontation caused by antimicrobial compounds and to exploitative competition caused by responses to preferred energy sources for their metabolic demands (Banerjee et al., 2018; Hassani et al., 2018). We observed that six OTUs affliated with

362 Aspergillaceae (Ascomycota) were classified as putative keystone taxa, and were mainly involved
363 in fungal-bacterial associations. The putative keystone OTUs from Aspergillaceae may secrete
364 antibiotics to maintain a high bonus from the "resource scramble" with bacteria. The strains of
365 Aspergillaceae (e.g., *Penicillium* and *Aspergillus*) have the ability to produce antibiotics, which
366 are an important part of microbial cross-kingdom warfare (Houbraken & Samson, 2011).
367 Our results indicated that bacterial-fungal associations had strong negative correlations with
368 bacterial diversity. The influences of negative associations on microbial diversity are affected by
369 intrinsic differences in the antagonistic abilities of the association partners. Microbial secondary
370 metabolites produced by the fungal community exert strong selective pressure on bacterial
371 diversity through membrane disruption, inhibition of cell wall biosynthesis and primary
372 metabolism, or disruption by quorum sensing signals (Getzke et al., 2019; Coller et al., 2019).
373 The fungus *Penicillium* can inhibit the proliferation and dispersal dynamics of competing bacteria
374 by producing antibiotics, thereby reducing bacterial diversity through antagonistic interactions
375 (Bahram et al., 2018; Zhang et al., 2018). Given the asymmetries in bacterial-fungal competition,
376 less adaptive bacterial taxa were more likely to be eliminated in the competitive interactions.
377 Strong asymmetric competition can induce the elimination of weaker competitive genotypes and
378 consequently reduce bacterial diversity (Guillemet et al., 2022). However, it should worth noting
379 that the link between bacterial-fungal associations and bacterial diversity is bidirectional rather
380 than unidirectional. Since potential bacterial-fungal competition can directly decrease bacterial
381 diversity, it is indeed bacterial diversity that determines the direction and strength of bacterial-
382 fungal interactions. We further showed that the keystone bacterial diversity increased with total
383 bacterial diversity and negative bacterial-fungal correlations. Keystone taxa with different

384 competitive strategies and trait expression can alter their morphology and metabolism, thereby
385 persisting against direct displacement or overgrowth in the bacterial community (Maynard et al.,
386 2017b). More importantly, keystone taxa are critical for maintaining soil microbial diversity and
387 overall ecosystem plasticity (Herren & McMahon, 2018). These findings highlight the importance
388 of keystone bacterial diversity within the microbial community in maintaining soil carbon
389 function and enhancing SOC dynamics in the forest ecosystem.
390
391 **Negative associations regulated the relationship between bacterial diversity and SOC**
392 **dynamics**
393 Elucidating the relationships between microbial diversity and SOC dynamics in *Eucalyptus*
394 plantations is crucial to elucidate the mechanism of the microbial community in regulating C
395 mineralization in artificial forests. The high biodiversity induced by potential bacterial-fungal
396 competition can improve ecosystem function in complex terrestrial ecosystems (Jiao et al., 2021b).
397 However, we found that the positive relationship between diversity and function was not
398 statistically supported when the negative bacterial-fungal associations were considered. In
399 particular, the negative bacterial-fungal associations may favor the negative relationships of
400 bacterial diversity with C-degrading enzymatic activities and C mineralization. Microbial
401 diversity combined with negative associations in the network mediates microbial respiration and
402 carbon use efficiency (Maynard et al., 2017a). The bacterial community exposed to the high
403 negative association with fungi may have a significantly high metabolic affinity for sucrase, BG,
404 and BX, which were involved in the degradation of carbohydrates, cellulose, and hemicellulose.
405 This result indicated that the antagonistic bacterial-fungal associations decreased bacterial

406 diversity and eventually improved the consumption of carbon resources and energy. We further
407 observed that keystone bacterial diversity was negatively correlated with C-degrading enzymatic
408 activities and C mineralization, supporting that the functional traits of keystone taxa are
409 particularly important in determining the relationship between microbial diversity and SOC
410 dynamics. These putative keystone taxa may have competitive traits and advantages to degrade
411 recalcitrant C and more efficiently capture limiting resources. Keystone taxa are often essential
412 for community functioning because they are responsible for carbon metabolic activities and C
413 mineralization (Lynch & Neufeld, 2015; Chen et al., 2019). However, we find that it is difficult
414 to provide empirical evidence for theoretical predictions about how keystone taxa orchestrate
415 microbial diversity to mediate ecosystem processes. Therefore, further research is needed to
416 manipulate specific keystone taxa to explore their ecological importance for the structure and
417 functioning of entire microbial communities.

418 Our study indicates that the decrease in bacterial diversity caused by negative bacterial-
419 fungal associations regulates SOC dynamics under successive planting of *Eucalyptus*, which is
420 usually overlooked in current management practices. Consistent with previous studies performed
421 in different regions (Xu et al., 2021; Dai et al., 2023), SOC degradation was observed after two
422 generations of successive planting of *Eucalyptus*. We found that the influences of *Eucalyptus*
423 planting on total bacterial and keystone bacterial diversity and bacterial-fungal associations relied
424 heavily on the generation of plantation. To prevent excessive SOC degradation in *Eucalyptus*
425 plantations, it is preferable to avoid multi-generational planting (particularly planting more than
426 two generations), and to prolong the rotation in *Eucalyptus* plantations that may undergo logging
427 in the short term. To advance the explanatory and predictive understanding of SOC dynamics in

forest ecosystems, it is crucial to investigate the role of temporal scale in mediating bacterial diversity through negative bacterial-fungal associations.

5 CONCLUSIONS

Our study advances previous knowledge on microbial diversity and the potential for cross-kingdom competition to mediate SOC storage in forest ecosystems. We provided empirical evidence that successive planting of *Eucalyptus* increased negative bacterial-fungal associations and improved C-degrading enzymatic activities and C mineralization by decreasing total bacterial and keystone bacterial diversity. By linking SOC mineralization to negative bacterial-fungal co-occurrence, our study provides a framework for uncovering mechanistic insights into the patterns and biochemical consequences of important bacterial-fungal associations in soil systems (**Fig. 6**). These results can be extended to determine how changes in cross-kingdom associations modulate SOC cycling dynamics in a variety of ecosystems.

REFERENCES

Bader, G. D., & Hogue, C. W. (2003). An automated method for finding molecular complexes in large protein interaction networks. BMC Bioinformatics, 4(1), 2. https://doi:10.1186/1471-2105-4-2

Bahram, M., Hildebrand, F., Forslund, S. K., Anderson, J. L., Soudzilovskaia, N. A., Bodegom, P. M., Bengtsson-Palme, J., Anslan, S., Coelho, L. P., Harend, H., Huerta-Cepas, J., Medema, M. H., Maltz, M. R., Mundra, S., Olsson, P. A., Pent, M., Polme, S., Sunagawa, S., Ryberg,

449 M., Tedersoo, L., & Bork, P. (2018). Structure and function of the global topsoil microbiome.
450 Nature, 560(7717), 233–237. https://doi:10.1038/s41586-018-0386-6
451 Banerjee, S., Schlaeppi, K., & van der Heijden, M. G. A. (2018). Keystone taxa as drivers of
452 microbiome structure and functioning. Nature Reviews Microbiology, 16(9), 567–576.
453 https://doi:10.1038/s41579-018-0024-1
454 Bastian, M., Heymann, S., & Jacomy, M. (2009). Gephi: An open source software for exploring
455 and manipulating networks: International AAAI conference on web and social media.
456 Bazzicalupo, A. L., Bálint, M., & Schmitt, I. (2013). Comparison of ITS1 and ITS2 rDNA in 454
457 sequencing of hyperdiverse fungal communities. Fungal Ecology, 6(1), 102–109.
458 https://doi:10.1016/j.funeco.2012.09.003
459 Becker, J., Eisenhauer, N., Scheu, S., & Jousset, A. (2012). Increasing antagonistic interactions
460 cause bacterial communities to collapse at high diversity. Ecology Letters, 15(5), 468–474.
461 https://doi:10.1111/j.1461-0248.2012.01759.x
462 Bell C.W., Fricks B.E., Rocca J.D., Steinweg J.W., McMahon S.K., & Wallenstein M.D. (2013)
463 High-throughput fluorometric measurement of potential soil extracellular enzyme activities.
464 Journal of Visualized Experiments, 81, e50961. https://doi.org/10.3791/50961
465 Berry, D., & Widder, S. (2014). Deciphering microbial interactions and detecting keystone
466 species with co-occurrence networks. Frontiers in Microbiology, 5, 1−14.
467 https://doi:10.3389/fmicb.2014.00219
468 Byrne, B. M. (2010). Structural equation modeling with AMOS: Basic concepts, applications,
469 and programming (2nd ed.). Routledge/Taylor & Francis Group.
470 Caporaso, J. G., Kuczynski, J., Stombaugh, J., Bittinger, K., Bushman, F. D., Costello, E. K.,

471 Fierer, N., Pena, A. G., Goodrich, J. K., Gordon, J. I., Huttley, G. A., Kelley, S. T., Knights,
472 D., Koenig, J. E., Ley, R. E., Lozupone, C. A., McDonald, D., Muegge, B. D., Pirrung, M.,
473 Reeder, J., Sevinsky, J. R., Tumbaugh, P. J., Walters, W. A., Widmann, J., Yatsunenko, T.,
474 Zaneveld, J., & Knight, R. (2010). QIIME allows analysis of high-throughput community
475 sequencing data. Nature Methods, 7(5), 335–336. https://doi:10.1038/nmeth.f.303
476 Cecilia, M., Fischer, H., & Tranvik, L. J. (2006). Antagonism between bacteria and fungi:
477 substrate competition and a possible tradeoff between fungal growth and tolerance towards
478 bacteria. Oikos, 113, 233−242. https://doi:10.2307/40234798
479 Chen, J., Feng, K., Hannula, S. E., Kuzyakov, Y., Li, Y., & Xu, H. (2021). Interkingdom plant-
480 microbial ecological networks under selective and clear cutting of tropical rainforest. Forest
481 Ecology and Management, 491, 119182. https://doi:10.1016/j.foreco.2021.119182
482 Chen, L., Liu, L., Mao, C., Qin, S., Wang, J., Liu, F., Blagodatsky, S., Yang, G. B., Zhang, Q.
483 W., Zhang, D. Y., Yu, J. C., & Yang, Y. (2018). Nitrogen availability regulates topsoil carbon
484 dynamics after permafrost thaw by altering microbial metabolic efficiency. Nature
485 Communications, 9(1), 3951. https://doi:10.1038/s41467-018-06232-y
486 Chen, L., Jiang, Y., Liang, C., Luo, Y., Xu, Q., Han, C., Zhao, Q., & Sun, B. (2019). Competitive
487 interaction with keystone taxa induced negative priming under biochar amendments.
488 Microbiome, 7(1), 77. https://doi:10.1186/s40168-019-0693-7
489 Coller, E., Cestaro, A., Zanzotti, R., Bertoldi, D., Pindo, M., Larger, S., Albanese, D., Mescalchin,
490 E., & Donati, C. (2019). Microbiome of vineyard soils is shaped by geography and
491 management. Microbiome, 7(1), 140. https://doi:10.1186/s40168-019-0758-7
492 Dai Q, Wang T, Wei P, & Fu Y. (2023). Effects of successive planting of eucalyptus plantations

493 on tree growth and soil quality. Sustainability, 15, 6746. https://doi.org/10.3390/su15086746.
494 De Boer, W. de, Folman, L. B., Summerbell, R. C., & Boddy, L. (2005). Living in a fungal world:
495 impact of fungi on soil bacterial niche development. FEMS Microbiology Reviews, 29(4),
496 795–811. https://doi:10.1016/j.femsre.2004.11.005
497 Deveau, A., Bonito, G., Uehling, J., Paoletti, M., Becker, M., Bindschedler, S., Hacqurd S., Herve
498 V., Labbe, J., Lastovetsky, O.A., Mieszkin, S., Millet, L. J., Vajna, B., Junier, P., Bonfante,
499 P., Krom, B.P., Olsson, S., van Elsas, J.D., & Wick, L. Y. (2018). Bacterial–fungal
500 interactions: ecology, mechanisms and challenges. FEMS Microbiology Reviews, 42(3),
501 335–352. https://doi:10.1093/femsre/fuy008
502 De Vries, F. T., Griffiths, R. I., Bailey, M., Craig, H., Girlanda, M., Gweon, H. S., Hallin, S.,
503 Kaisermann, A., Keith, A. M., Kretzschmar, M., Lemanceau, P., Lumini, E., Mason, K. E.,
504 Oliver, A., Ostle, N., Prosser, J. I., Thion, C., Thomson, B., & Bardgett, R. D. (2018). Soil
505 bacterial networks are less stable under drought than fungal networks. Nature
506 Communications, 9(1), 3033. https://doi:10.1038/s41467-018-05516-7
507 Durán, P., Thiergart, T., Garrido-Oter, R., Agler, M., Kemen, E., Schulze-Lefert, P., & Hacquard,
508 S. (2018). Microbial interkingdom interactions in roots promote Arabidopsis survival. Cell,
509 175(4), 973–983.e14. https://doi:10.1016/j.cell.2018.10.020
510 Edgar, R. C., Haas, B. J., Clemente, J. C., Quince, C., & Knight, R. (2011). UCHIME improves
511 sensitivity and speed of chimera detection. Bioinformatics, 27(16), 2194–2200.
512 https://doi:10.1093/bioinformatics/btr381
513 Fan, K., Delgado-Baquerizo, M., Guo, X., Wang, D., Zhu, Y., & Chu, H. (2021). Biodiversity of
514 key-stone phylotypes determines crop production in a 4-decade fertilization experiment. The

515 ISME Journal, 15, 550−561. https://doi:10.1038/s41396-020-00796-8

516 Falagán, C., & Johnson, D. B. (2014). *Acidibacter ferrireducens* gen. nov., sp. nov.: an acidophilic
517 ferric iron-reducing gammaproteobacterium. Extremophiles, 18(6), 1067–1073.
518 https://doi:10.1007/s00792-014-0684-3

519 Feng, K., Peng, X., Zhang, Z., Gu, S. S., He, Q., Shen, W., & Deng, Y. (2022). iNAP: An
520 integrated network analysis pipeline for microbiome studies. iMeta, 1(2), e13.
521 https://doi.org/10.1002/imt2.13

522 Friedman, J., & Alm, E. J. (2012). Inferring correlation networks from genomic survey data. PLoS
523 Computational Biology, 8(9), e1002687. https://doi:10.1371/journal.pcbi.1002687

524 Getzke, F., Thiergart, T., & Hacquard, S. (2019). Contribution of bacterial-fungal balance to plant
525 and animal health. Current Opinion in Microbiology, 49, 66–72.
526 https://doi:10.1016/j.mib.2019.10.009

527 Ghoul, M., & Mitri, S. (2016). The ecology and evolution of microbial competition. Trends in
528 Microbiology, 24(10), 833–845. https://doi:10.1016/j.tim.2016.06.011

529 Grömping, U. (2006). Relative importance for linear regression in R: the package relaimpo.
530 Journal of Statistical Software, 17(1), 1-27. https://doi.org/10.18637/jss.v017.i01

531 Guillaume, T., Damris, M., & Kuzyakov, Y. (2015). Losses of soil carbon by converting tropical
532 forest to plantations: erosion and decomposition estimated by $\delta^{13}C$. Global Change Biology,
533 21(9), 3548–3560. https://doi:10.1111/gcb.12907

534 Guillemet, M., Chabas, H., Nicot, A., Gatchich, F., Ortega-Abboud, E., Buus, C., Hindhede, L.,
535 Rousseau, G., Bataillon, T., Moineau, S., & Gandon, S. (2022). Competition and coevolution
536 drive the evolution and the diversification of CRISPR immunity. Nature Ecology and

537 Evolution, 21, 3548−3560. https://doi.org/10.1038/s41559-022-01841-9.

538 Hassani, M. A., Durán, P., & Hacquard, S. (2018). Microbial interactions within the plant
539 holobiont. Microbiome, 6(1), 58. https://doi:10.1186/s40168-018-0445-0

540 He, Y., Caporaso, J. G., Jiang, X.-T., Sheng, H.-F., Huse, S. M., Rideout, J. R., Edgar, R. C.,
541 Kopylova, E., Walters, W. A., Knight, R., & Zhou, H. W. (2015). Stability of operational
542 taxonomic units: an important but neglected property for analyzing microbial diversity.
543 Microbiome, 3(1), 20. https://doi:10.1186/s40168-015-0081-x

544 Herren, C. M., & McMahon, K. D. (2018). Keystone taxa predict compositional change in
545 microbial communities. Environmental Microbiology, 20(6), 2207–2217.
546 https://doi:10.1111/1462-2920.14257

547 Houbraken, J., & Samson, R. A. (2011). Phylogeny of Penicillium and the segregation of
548 Trichocomaceae into three families. Studies in Mycology, 70, 1–51.
549 https://doi:10.3114/sim.2011.70.01

550 Hunter, I. (2001). Above ground biomass and nutrient uptake of three tree species (Eucalyptus
551 camaldulensis, Eucalyptus grandis and Dalbergia sissoo) as affected by irrigation and
552 fertiliser, at 3 years of age, in southern India. Forest Ecology and Management, 144(1-3),
553 189–200. https://doi:10.1016/s0378-1127(00)00373-x

554 Ismaw S.M., Gandaseca S., & Ahmed O.H. (2012) Effects of deforestation on soil major macro-
555 nutrient and other selected chemical properties of secondary tropical peat swamp forest. Int.
556 J. Phys. Sci. 7, 2225–2228. https://doi.org/10.5897/IJPS11.596

557 Jenkinson, D. S., & Powlson, D. S. (1976). The effects of biocidal treatments on metabolism in
558 soil-V. Soil Biology and Biochemistry, 8(3), 209–213. https://doi:10.1016/0038-

559 0717(76)90005-5

560 Jiao S, Lu Y, & Wei G. (2021a). Soil multitrophic network complexity enhances the link between
561 biodiversity and multifunctionality in agricultural systems. Global Chang Biology, 28: 140-
562 153. https://doi.org/10.1111/gcb.15917

563 Jiao, S., Peng, Z., Qi, J., Gao, J., & Wei, G. (2021b). Linking bacterial-fungal relationships to
564 microbial diversity and soil nutrient cycling. mSystems, 6, e01052−20.
565 https://10.1128/mSystems.01052-20

566 Kõljalg, U., Nilsson, R. H., Abarenkov, K., Tedersoo, L., Taylor, A. F. S., Bahram, M., Bates,
567 S.T., Bruns, T. D., Bengtsson-Palme, J., Callaghan, T. M., Douglas, B., Drenkhan, T.,
568 Eberhardt, U., Duenas, M., Grebenc, T., Griffith, G. W., Hartmann, M., Kirk, P. M., Kohout,
569 P., Larsson, E., Lindahl, B. D., Luecking, R., Martin, M. P., Matheny, P. B., Nguyen, N. H.,
570 Niskanen, T., Oja, J., Peay, K. G., Peintner, U., Peterson, M., Poldmaa, K., Saag, L., Saar,
571 I., Schuessler, A., Scott, J. A., Senes, C., Smith, M. E., Suija, A., Taylor, D. L., Telleria, M.
572 T., Weiss, M., & Larsson, K. H. (2013). Towards a unified paradigm for sequence-based
573 identification of fungi. Molecular Ecology, 22(21), 5271–5277.
574 https://doi:10.1111/mec.12481

575 Lee, C. K., Barbier, B. A., Bottos, E. M., McDonald, I. R., & Cary, S. C. (2012). The inter-valley
576 soil comparative survey: the ecology of dry valley edaphic microbial communities. The
577 ISME Journal, 6(5), 1046–1057. https://doi:10.1038/ismej.2011.170

578 Lehmann, J., & Kleber, M. (2015). The contentious nature of soil organic matter. Nature, 528,
579 60–68. https://doi:10.1038/nature16069

580 Luo, G., Sun, B., Li, L., Li, M., Liu, M., Zhu, Y., Guo, S., Ling, N., & Shen, Q. (2019).

581 Understanding how long-term organic amendments increase soil phosphatase activities:
582 Insight into phoD- and phoC-harboring functional microbial populations. Soil Biology and
583 Biochemistry, 139, 107632. https://doi:10.1016/j.soilbio.2019.107632
584 Lustenhouwer, N., Maynard, D. S., Bradford, M. A., Lindner, D. L., Oberle, B., Zanne, A. E., &
585 Crowther, T. W. (2020). A trait-based understanding of wood decomposition by fungi.
586 Proceedings of the National Academy of Sciences, 117(21), 11551–11558.
587 https://doi:10.1073/pnas.1909166117
588 Lynch, M. D. J., & Neufeld, J. D. (2015). Ecology and exploration of the rare biosphere. Nature
589 Reviews Microbiology, 13(4), 217–229. https://doi:10.1038/nrmicro3400
590 Ma, B., Wang, H., Dsouza, M., Lou, J., He, Y., Dai, Z., Brookes, P.C., Xu, J., & Gilbert, J. A.
591 (2016). Geographic patterns of co-occurrence network topological features for soil
592 microbiota at continental scale in eastern China. The ISME Journal, 10: 1891–1901.
593 https://doi.org/10.1038/ismej.2015.261
594 Manju, S., & Singh Chadha, B. (2011). Production of hemicellulolytic enzymes for hydrolysis of
595 lignocellulosic biomass. Biofuels, 203–228. https://doi:10.1016/b978-0-12-385099-
596 7.00009-7
597 Maynard, D. S., Crowther, T. W., & Bradford, M. A. (2017a). Competitive network determines
598 the direction of the diversity–function relationship. Proceedings of the National Academy of
599 Sciences, 114(43), 11464–11469. https://doi:10.1073/pnas.1712211114
600 Maynard, D. S., Bradford, M. A., Lindner, D. L., van Diepen, L. T. A., Frey, S. D., Glaeser, J. A.,
601 & Crowther, T. W. (2017b). Diversity begets diversity in competition for space. Nature
602 Ecology & Evolution, 1(6), 0156. https://doi:10.1038/s41559-017-0156

603 Maynard, D. S., Bradford, M. A., Covey, K. R., Lindner, D., Glaeser, J., Talbert, D. A., Tinker,
604 P.J., Walker, D. M., & Crowther, T. W. (2019). Consistent trade-offs in fungal trait
605 expression across broad spatial scales. Nature Microbiology, 4(5), 846–853.
606 https://doi:10.1038/s41564-019-0361-5
607 Mille-Lindblom, C., & Tranvik, L. J. (2003). Antagonism between bacteria and fungi on
608 decomposing aquatic plant litter. Microbial Ecology, 45(2), 173–182.
609 https://doi:10.1007/s00248-002-2030-z
610 Mori, A. S., Cornelissen, J. H. C., Fujii, S., Okada, K., & Isbell, F. (2020). A meta-analysis on
611 decomposition quantifies afterlife effects of plant diversity as a global change driver. Nature
612 Communications, 11(1), 4547. https://doi:10.1038/s41467-020-18296-w
613 Mould, D. L., & Hogan, D. A. (2021). Intraspecies heterogeneity in microbial interactions.
614 Current Opinion in Microbiology, 62, 14–20. https://doi:10.1016/j.mib.2021.04.003
615 Olesen, J. M., Bascompte, J., Dupont, Y. L., & Jordano, P. (2007). The modularity of pollination
616 networks. Proceedings of the National Academy of Sciences, 104(50), 19891–19896.
617 https://doi:10.1073/pnas.0706375104
618 Pearce, D. A., Newsham, K. K., Thorne, M. A. S., Calvo-Bado, L., Krsek, M., Laskaris, P.,
619 Hodson, A., & Wellington, E. M. (2012). Metagenomic analysis of a southern maritime
620 Antarctic soil. Frontiers in Microbiology, 3. https://doi:10.3389/fmicb.2012.00403
621 Quast, C., Pruesse, E., Yilmaz, P., Gerken, J., Schweer, T., Yarza, P., Peplies, J., & Glöckner, F.
622 O. (2013). The SILVA ribosomal RNA gene database project: improved data processing and
623 web-based tools. Nucleic Acids Research, 41(D1), D590–D596.
624 https://doi:10.1093/nar/gks1219

625 Ribeiro, H. M., Fangueiro, D., Alves, F., Vasconcelos, E., Coutinho, J., Bol, R., & Cabral, F.
626 (2010). Carbon-mineralization kinetics in an organically managed Cambic Arenosol
627 amended with organic fertilizers. Journal of Plant Nutrition and Soil Science, 173(1), 39–
628 45. https://doi:10.1002/jpln.200900015
629 Ruan, C. J., Ramoneda, J., Gogia, G., Wang, G., & Johnson, D. (2022). Fungal hyphae regulate
630 bacterial diversity and plasmid-mediated functional novelty during range expansion. Current
631 Biology, 4131646. https://doi10.1016/j.cub.2022.11.009
632 Sokol, N. W., Slessarev, E., Marschmann, G. L., Nicolas, A., Blazewicz, S. J., Brodie, E. L.,
633 Firestone, M. K., Foley, M. M., Hestrin, R., Hungate, B. A., Koch, B. J., Stone, B. W.,
634 Sullivan, M. B., Zablocki, O., Trubl, G., McFarlane, K., Stuart, R., Nuccio, E., & Weber, P.
635 (2022). Life and death in the soil microbiome: how ecological processes influence
636 biogeochemistry. Nature Reviews Microbiology, 20, 415−430.
637 https://doi.org/10.1038/s41579-022-00695-z
638 Sparks, D. L., Page, A. L., Helmke, P. A., Loeppert, R. H., Soltanpour, P. N., Tabatabai, M. A.,
639 Johnston, C. T., & Sumner, M. E. (1996). Methods of Soil Analysis. SSSA Book Series.
640 https://doi:10.2136/sssabookser5.3
641 Temesgen, D., Gonzálo, J., & Turri ó n, M. B. (2016). Effects of short-rotation *Eucalyptus*
642 plantations on soil quality attributes in highly acidic soils of the central highlands of Ethiopia.
643 Soil Use and Management, 32(2), 210–219. https://doi:10.1111/sum.12257
644 Trivedi, P., Leach, J. E., Tringe, S. G., Sa, T., & Singh, B. K. (2020). Plant–microbiome
645 interactions: from community assembly to plant health. Nature Reviews Microbiology,
646 18(11), 607–621. https://doi:10.1038/s41579-020-0412-1

647 Van der Heijden, M. G., Bruin, S. de, Luckerhoff, L., van Logtestijn, R. S., & Schlaeppi, K.
648 (2016). A widespread plant-fungal-bacterial symbiosis promotes plant biodiversity, plant
649 nutrition and seedling recruitment. The ISME Journal, 10(2), 389–399.
650 https://doi:10.1038/ismej.2015.120
651 Veldkamp E., Schmidt M., Powers J.S., & Corre M.D. (2020). Deforestation and reforestation
652 impacts on soils in the tropics. Nature Review Earth and Environment, 1, 590–605.
653 https://doi.org/10.1038/s43017-020-0091-5
654 Xu Y., Du A., Wang Z., Zhu W., Li C., & Wu L. (2020). Effects of different rotation periods of
655 Eucalyptus plantations on soil physiochemical properties, enzyme activities, microbial
656 biomass and microbial community structure and diversity. Forest Ecology and Management,
657 456, 117683. https://doi.org/10.1016/j.foreco.2021.119877
658 Xu, Y., Ren, S., Liang, Y., Du, A., Li, C., Wang, Z., Zhu, W., & Wu, L. (2021). Soil nutrient
659 supply and tree species drive changes in soil microbial communities during the
660 transformation of a multi-generation *Eucalyptus* plantation. Applied Soil Ecology, 166,
661 103991. https://doi:10.1016/j.apsoil.2021.103991
662 Yang, Y., Chen, H., Gao, H., & An, S. (2019). Response and driving factors of soil microbial
663 diversity related to global nitrogen addition. Land Degradation & Development, 31, 190−204.
664 https://doi:10.1002/ldr.3439
665 Zhang, Y., & Sun, Y. (2011). HMM-FRAME: accurate protein domain classification for
666 metagenomic sequences containing frameshift errors. BMC Bioinformatics, 12(1), 198.
667 https://doi:10.1186/1471-2105-12-198
668 Zhang, X., Liu, S., Wang, J., Huang, Y., Freedman, Z., Fu, S., Liu, K., Wang, H., Li, X., Yao,

669 M., Liu, X., & Schuler, J. (2020). Local community assembly mechanisms shape soil
670 bacterial β diversity patterns along a latitudinal gradient. Nature Communications, 11(1),
671 5428. https://doi:10.1038/s41467-020-19228-4
672 Zhang, Y., Kastman, E. K., Guasto, J. S., & Wolfe, B. E. (2018). Fungal networks shape dynamics
673 of bacterial dispersal and community assembly in cheese rind microbiomes. Nature
674 Communications, 9(1), 336. https://doi:10.1038/s41467-017-02522-z
675 Zhu, L., Wang, X., Chen, F., Li, C., & Wu, L. (2019). Effects of the successive planting of
676 Eucalyptus urophylla on the soil bacterial and fungal community structure, diversity,
677 microbial biomass, and enzyme activity. Land Degradation & Development, 30, 636−646.
678 https://doi:10.1002/ldr.3249

679

680

681 **Figure captions**

682 **FIGURE 1** Soil organic carbon content (a), carbon mineralization (b) and enzymatic activities
683 (c). Bars with different lowercase letters indicate significant differences ($P < 0.05$). PrG, first
684 generation of *Eucalyptus*; SeG, secondary generation of *Eucalyptus*, ThG, third generation of
685 *Eucalyptus*; FoG, fourth generation of *Eucalyptus*; CK, evergreen broadleaf forest as control.
686 **FIGURE 2** Changes in soil bacterial (a) and fungal (b) diversity with successive planting of
687 *Eucalyptus*, and the contribution of soil properties to bacterial and fungal diversity and microbial
688 biomass based on correlation and best multiple regression model (c). Circle size represents
689 variable importance (proportion of variability explained by multiple regression modeling and
690 variance decomposition analysis). Colors represent Spearman's correlations. BD, bulk density;

691 Pt, total porosity; Pa, aeration porosity; CEC, cation exchange capacity; TN, total nitrogen; TP,
692 total phosphorus; TK, total potassium; NH_4^+−N, ammonium nitrogen; NO_3^-−N, nitrate nitrogen;
693 AP, available phosphorus; AK, available potassium; MBC: microbial biomass carbon; MBN:
694 microbial biomass nitrogen; MBP: microbial biomass phosphorus. PrG, first generation of
695 *Eucalyptus*; SeG, secondary generation of *Eucalyptus*, ThG, third generation of *Eucalyptus*; FoG,
696 fourth generation of *Eucalyptus*; CK, evergreen broadleaf forest as control. ** $P < 0.01$; * $P <$
697 0.05.

698 **FIGURE 3** The bacterial-fungal co-occurrence network across all samples. (a) The nodes and
699 edges of the network are colored by the modules. (b) The nodes and edges of the network are
700 colored by the bacterial and fungal phyla. The proportion of nodes and edges the bacterial-fungal
701 network (c). A connection stand for a significant ($P < 0.05$) correlation between two OTUs. The
702 size of each node is proportional to the number of connections, and the thickness of each
703 connection between two nodes is proportional to the weight of the correlation. BF_N, bacterial-
704 fungal negative associations; BF_P, bacterial-fungal positive associations; FF_N, fungal-fungal
705 negative associations; FF_P, fungal-fungal positive associations; BB_N, bacterial-bacterial
706 negative associations; BB_P, bacterial-bacterial positive associations. NPP, The proportion of
707 negative edges to positive edges; BBA, bacterial-bacterial associations; FFA, fungal-fungal
708 associations; BFA, bacterial-fungal associations. PrG, first generation of *Eucalyptus*; SeG,
709 secondary generation of *Eucalyptus*, ThG, third generation of *Eucalyptus*; FoG, fourth generation
710 of *Eucalyptus*; CK, evergreen broadleaf forest as control.

711 **FIGURE 4** Z_i-P_i plot showed the distribution of keystone taxa (a) based on their topological roles.
712 The threshold values of Z_i and P_i for categorizing OTUs were 2.5 and 0.62 respectively. (b) The

713 diversity of bacterial and fungal keystone taxa indicated by Shannon index and Chao1 richness.
714 Nodes in the network can be classified into network hubs ($Z_i > 0.25$, $P_i > 0.62$;), module hubs (Z_i
715 > 0.25, $P_i \leq 0.62$;), connectors ($Z_i \leq 0.25$, $P_i > 0.62$), and peripherals ($Z_i \leq 0.25$, $P_i \leq 0.62$). Z_i, the
716 within-module connectivity; P_i, the among-module connectivity. Lowercase letters indicate the
717 significant difference among treatments at $P < 0.05$. PrG, first generation of *Eucalyptus*; SeG,
718 secondary generation of *Eucalyptus*, ThG, third generation of *Eucalyptus*; FoG, fourth generation
719 of *Eucalyptus*; CK, evergreen broadleaf forest as control.

720 **FIGURE 5** The impacts of soil properties, and bacterial and fungal community on carbon
721 mineralization using the structural equation modeling (a) and its standard total effects on soil
722 enzymatic activity (b) and carbon mineralization (c). Soil properties are represented by soil pH,
723 total nitrogen, and NH_4^+−N. The bacterial diversities are represented by Shannon index, and the
724 bacterial-fungal associations are represented by the proportion of negative bacterial-fungal
725 associations. Enzymatic activities represented by the activity of β-1,4-glucosidase (BG), β-
726 xylosidase (BX), and sucrase. Blue lines indicate positive relationships, while red lines indicate
727 negative relationships. The width of arrows indicates the strength of significant standardized path
728 coefficients ($P < 0.05$). Paths with non-significant coefficients are presented as gray line. *** P
729 < 0.001; ** $P < 0.01$; * $P < 0.05$.

730 **FIGURE 6** Conceptual figure of bacterial-fungal associations impacts on SOC decomposition in
731 successive planting of *Eucalyptus*. Successive planting of *Eucalyptus* decreased soil fertility and
732 induced the high degree of bacterial-fungal negative associations. The potential bacterial-fungal
733 competition led to the decline in the diversity of total and keystone bacteria, thereby improving
734 carbon (C) mineralization and C-degrading enzymatic activities. PrG, first generation of

735 *Eucalyptus*; SeG, secondary generation of *Eucalyptus*, ThG, third generation of *Eucalyptus*; FoG,

736 fourth generation of *Eucalyptus*; CK, evergreen broadleaf forest as control.

Table 1 Soil propertieis across successive planting of *Eucalyptus*

	CK	PrG	SeG	ThG	FoG
BD (g cm^{-3})	0.96±0.04ab	1.02±0.06ab	0.90±0.02b	0.98±0.08ab	1.08±0.07a
Pt (%)	50.37±2.22a	50.00±0.89a	53.61±2.79a	49.51±2.36a	51.50±2.32a
Pa (%)	20.76±4.33a	21.82±3.44a	20.91±4.23a	19.26±3.97a	18.76±2.46a
pH	4.47±0.02a	4.37±0.02b	4.29±0.02c	4.40±0.01b	4.24±0.01d
CEC(cmol kg^{-1})	15.92±0.81c	19.80±1.46ab	21.77±1.21a	17.34±1.81bc	17.55±0.77bc
TN (g kg^{-1})	2.58±0.07a	1.71±0.16c	2.25±0.11b	1.99±0.09bc	1.85±0.09c
TP (g kg^{-1})	0.52±0.03a	0.39±0.04bc	0.46±0.01b	0.39±0.03bc	0.36±0.04c
TK (g kg^{-1})	28.23±0.47a	21.83±1.47b	28.50±1.78a	23.23±0.64b	14.58±0.55c
NH_4^+-N (mg kg^{-1})	26.44±1.22a	10.44±0.77c	15.69±0.37b	10.03±0.20c	7.74±0.80d
NO_3^--N (mg kg^{-1})	1.98±0.52a	1.46±0.34ab	1.27±0.29ab	0.88±0.30b	1.03±0.18b
AP (mg kg^{-1})	5.96±0.97a	2.92±0.26b	5.20±0.60a	2.12±0.13b	1.97±0.13b
AK (mg kg^{-1})	97.83±7.37a	60.67±7.18b	71.83±7.09b	70.17±4.51b	66.00±6.76b

Numbers within rows followed by same lowercase letters indicate no differences among treatments, while different lowercase letters indicate differences among treatments ($p \leq 0.05$); BD:bulk density; Pt: total porosity; Pa: aeration porosity; CEC: cation exchange capacity; TN: total nitrogen; TP: total phosphorus; TK: total potassium; NH_4^+-N: ammonium nitrogen; NO_3^--N: nitrate nitrogen; AP: available phosphorus; AK: available potassium.

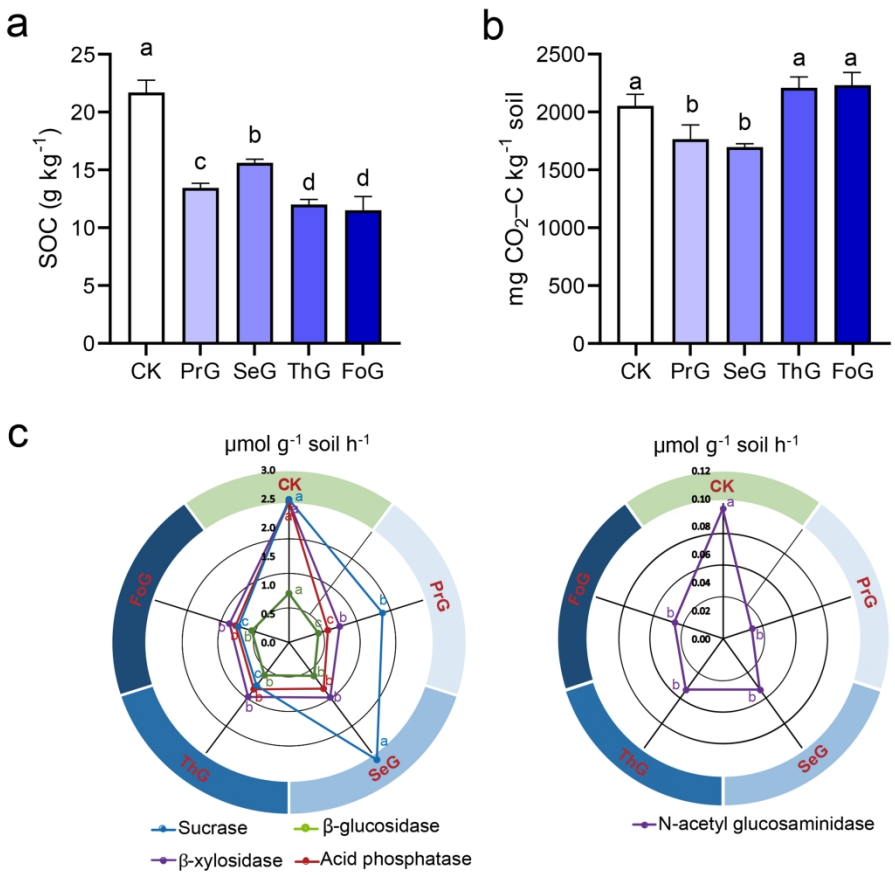

FIGURE 1 Soil organic carbon content (a), carbon mineralization (b) and enzymatic activities (c). Bars with different lowercase letters indicate significant differences ($P < 0.05$). PrG, first generation of Eucalyptus; SeG, secondary generation of Eucalyptus, ThG, third generation of Eucalyptus; FoG, fourth generation of Eucalyptus; CK, evergreen broadleaf forest as control.

1017x893mm (118 x 118 DPI)

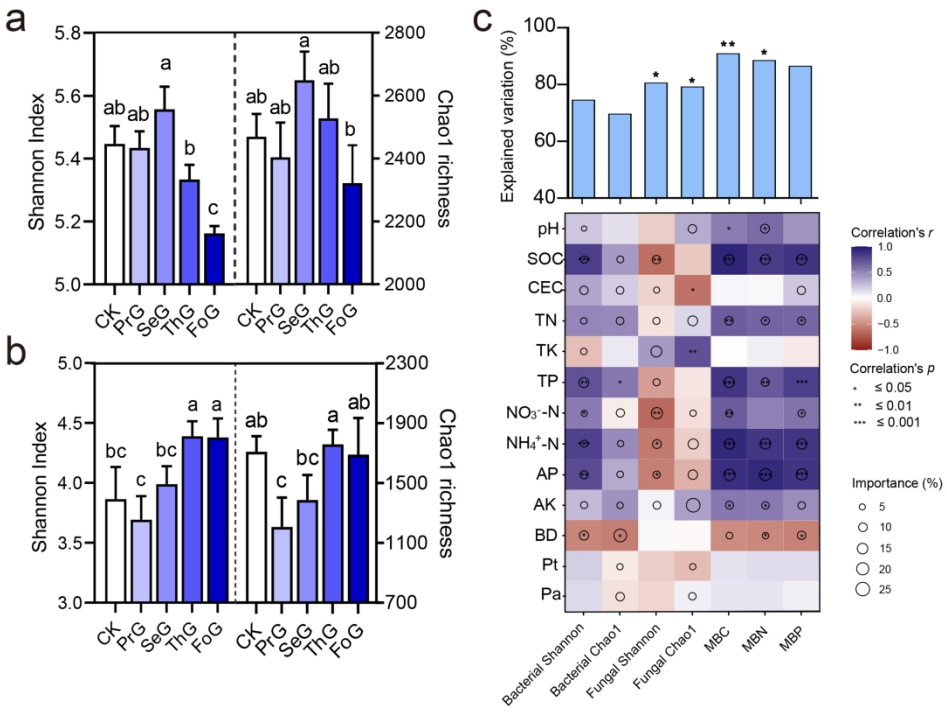

FIGURE 2 Changes in soil bacterial (a) and fungal (b) diversity with successive planting of Eucalyptus, and the contribution of soil properties to bacterial and fungal diversity and microbial biomass based on correlation and best multiple regression model (c). Circle size represents variable importance (proportion of variability explained by multiple regression modeling and variance decomposition analysis). Colors represent Spearman's correlations. BD, bulk density; Pt, total porosity; Pa, aeration porosity; CEC, cation exchange capacity; TN, total nitrogen; TP, total phosphorus; TK, total potassium; NH4+−N, ammonium nitrogen; NO3−−N, nitrate nitrogen; AP, available phosphorus; AK, available potassium; MBC: microbial biomass carbon; MBN: microbial biomass nitrogen; MBP: microbial biomass phosphorus. PrG, first generation of Eucalyptus; SeG, secondary generation of Eucalyptus, ThG, third generation of Eucalyptus; FoG, fourth generation of Eucalyptus; CK, evergreen broadleaf forest as control. ** P < 0.01; * P < 0.05.

1066x790mm (118 x 118 DPI)

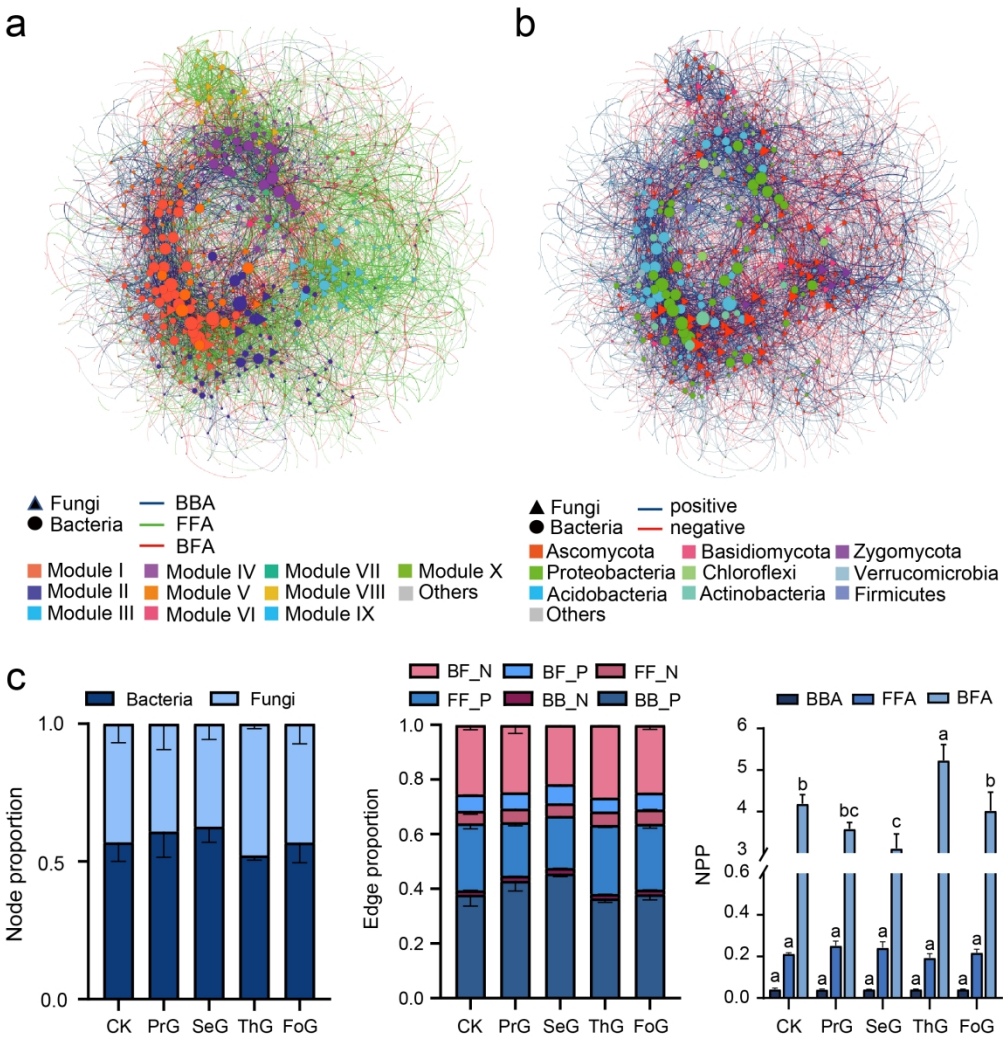

FIGURE 3 The bacterial-fungal co-occurrence network across all samples. (a) The nodes and edges of the network are colored by the modules. (b) The nodes and edges of the network are colored by the bacterial and fungal phyla. The proportion of nodes and edges the bacterial-fungal network (c). A connection stand for a significant ($P < 0.05$) correlation between two OTUs. The size of each node is proportional to the number of connections, and the thickness of each connection between two nodes is proportional to the weight of the correlation. BF_N, bacterial-fungal negative associations; BF_P, bacterial-fungal positive associations; FF_N, fungal-fungal negative associations; FF_P, fungal-fungal positive associations; BB_N, bacterial-bacterial negative associations; BB_P, bacterial-bacterial positive associations. NPP, The proportion of negative edges to positive edges; BBA, bacterial-bacterial associations; FFA, fungal-fungal associations; BFA, bacterial-fungal associations. PrG, first generation of Eucalyptus; SeG, secondary generation of Eucalyptus, ThG, third generation of Eucalyptus; FoG, fourth generation of Eucalyptus; CK, evergreen broadleaf forest as control.

539x559mm (118 x 118 DPI)

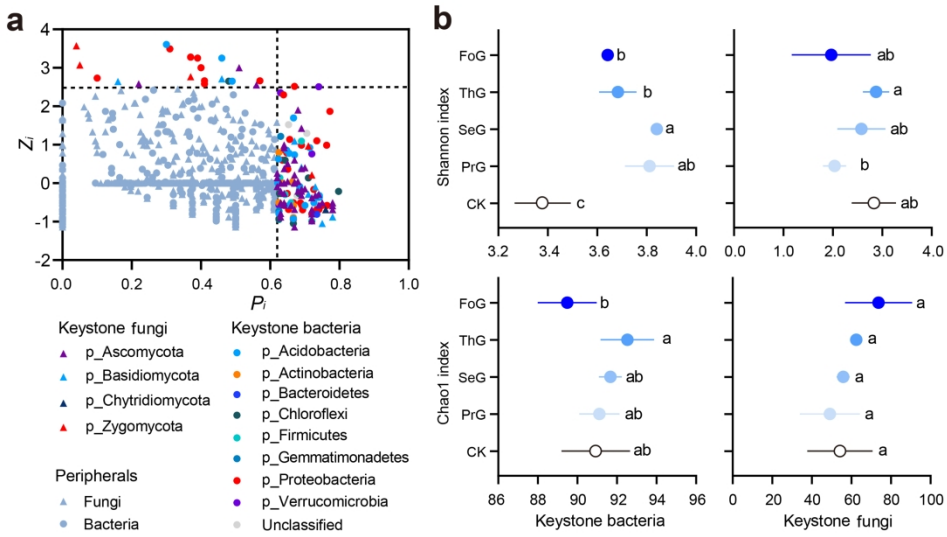

FIGURE 4 Zi-Pi plot showed the distribution of keystone taxa (a) based on their topological roles. The threshold values of Zi and Pi for categorizing OTUs were 2.5 and 0.62 respectively. (b) The diversity of bacterial and fungal keystone taxa indicated by Shannon index and Chao1 richness. Nodes in the network can be classified into network hubs (Zi > 0.25, Pi > 0.62;), module hubs (Zi > 0.25, Pi ≤ 0.62;), connectors (Zi ≤ 0.25, Pi > 0.62), and peripherals (Zi ≤ 0.25, Pi ≤ 0.62). Zi, the within-module connectivity; Pi, the among-module connectivity. Lowercase letters indicate the significant difference among treatments at P < 0.05. PrG, first generation of Eucalyptus; SeG, secondary generation of Eucalyptus, ThG, third generation of Eucalyptus; FoG, fourth generation of Eucalyptus; CK, evergreen broadleaf forest as control.

972x536mm (118 x 118 DPI)

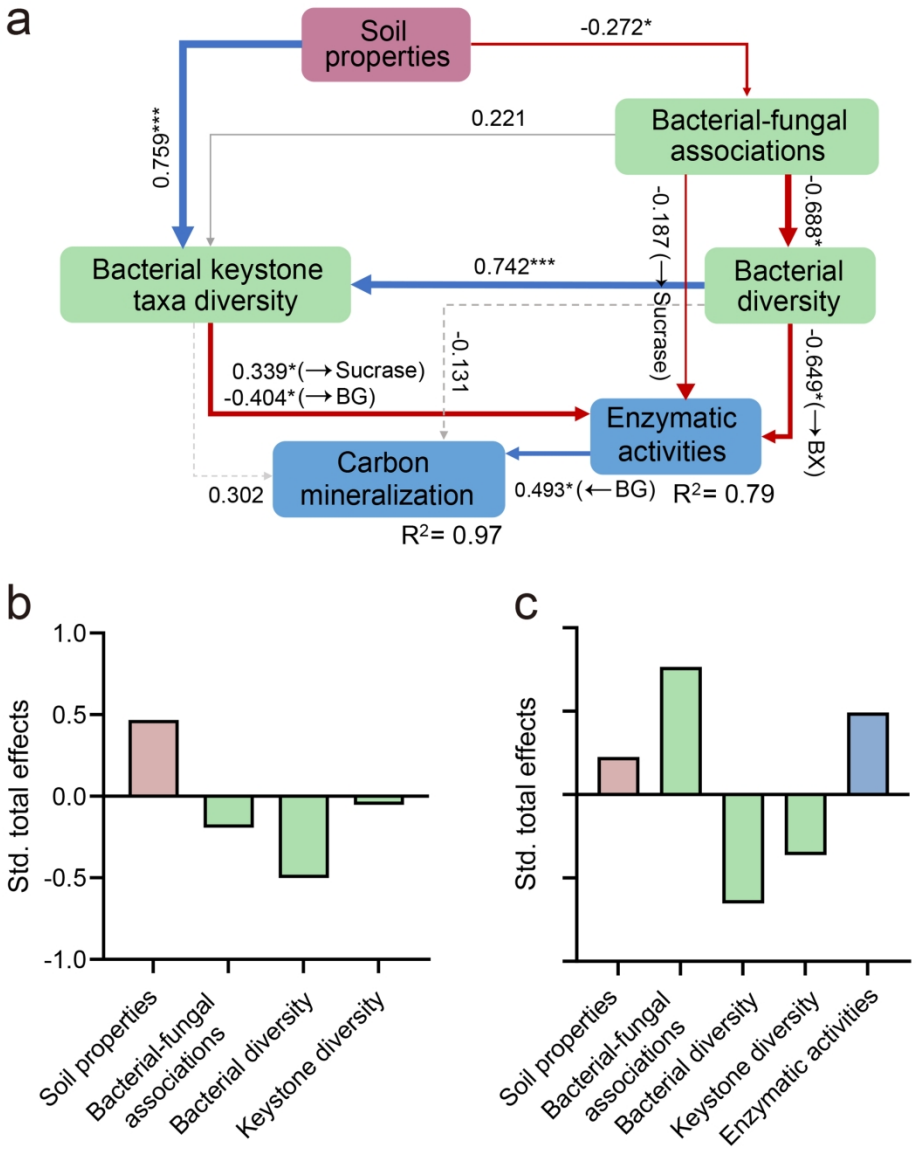

FIGURE 5 The impacts of soil properties, and bacterial and fungal community on carbon mineralization using the structural equation modeling (a) and its standard total effects on soil enzymatic activity (b) and carbon mineralization (c). Soil properties are represented by soil pH, total nitrogen, and NH4+−N. The bacterial diversities are represented by Shannon index, and the bacterial-fungal associations are represented by the proportion of negative edges to positive edges between bacteria and fungi. Enzymatic activities represented by the activity of β-1,4-glucosidase (BG), β-xylosidase (BX), and sucrase. Blue lines indicate positive relationships, while red lines indicate negative relationships. The width of arrows indicates the strength of significant standardized path coefficients ($P < 0.05$). Paths with non-significant coefficients are presented as gray line. *** $P < 0.001$; ** $P < 0.01$; * $P < 0.05$.

988x1222mm (118 x 118 DPI)

FIGURE 6 Conceptual figure of bacterial-fungal associations impacts on SOC decomposition in successive planting of Eucalyptus. Successive planting of Eucalyptus decreased soil fertility and induced the high degree of bacterial-fungal negative associations. The potential bacterial-fungal competition led to the decline in the diversity of total and keystone bacteria, thereby improving carbon (C) mineralization and C-degrading enzymatic activities. PrG, first generation of Eucalyptus; SeG, secondary generation of Eucalyptus, ThG, third generation of Eucalyptus; FoG, fourth generation of Eucalyptus; CK, evergreen broadleaf forest as control.

956x821mm (118 x 118 DPI)

Supplementary Materials for

Integrating variation in bacterial-fungal co-occurrence network with soil carbon dynamics

This file includes:

Figures S1 to S4

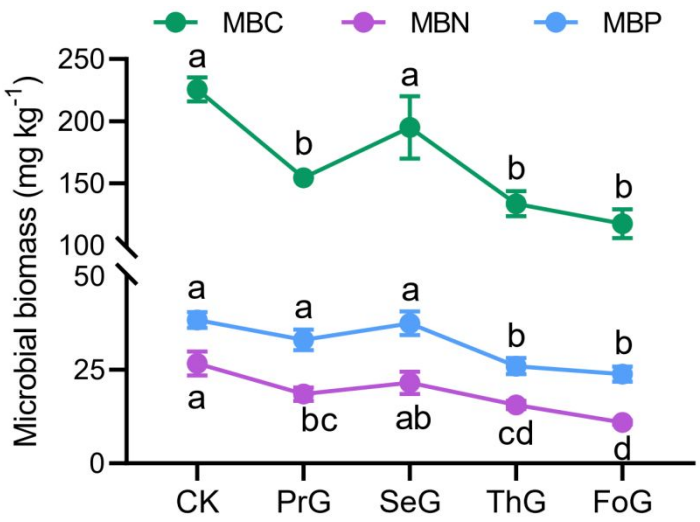

FIGURE S1 Microbial biomass determined by microbial biomass carbon (MBC), microbial biomass nitrogen (MBN) and microbial biomass phosphorus (MBP) in four generations of *Eucalyptus* plantations and evergreen broadleaf forest. Lowercase letters indicate the significant difference among treatments at $P < 0.05$. PrG, first generation of *Eucalyptus*; SeG, secondary generation of *Eucalyptus*, ThG, third generation of *Eucalyptus*; FoG, fourth generation of *Eucalyptus*; CK, evergreen broadleaf forest as control.

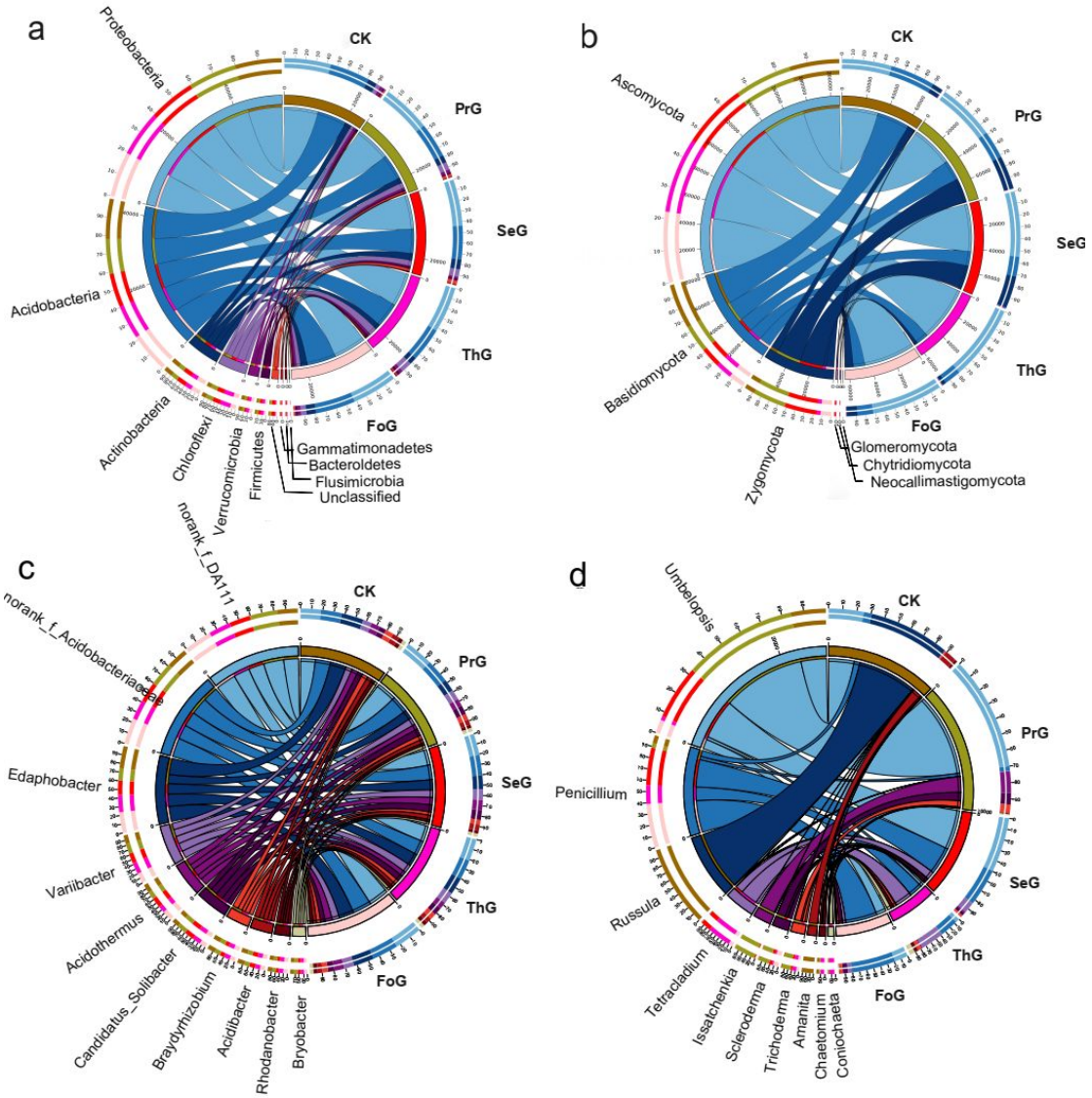

FIGURE S2. Relative abundance of dominant phyla/genera in the bacterial (a, c) and fungal communities (b, d) in four generations of *Eucalyptus* plantations and evergreen broadleaf forest. PrG, first generation of *Eucalyptus*; SeG, secondary generation of *Eucalyptus*, ThG, third generation of *Eucalyptus*; FoG, fourth generation of *Eucalyptus*; CK, evergreen broadleaf forest as control.

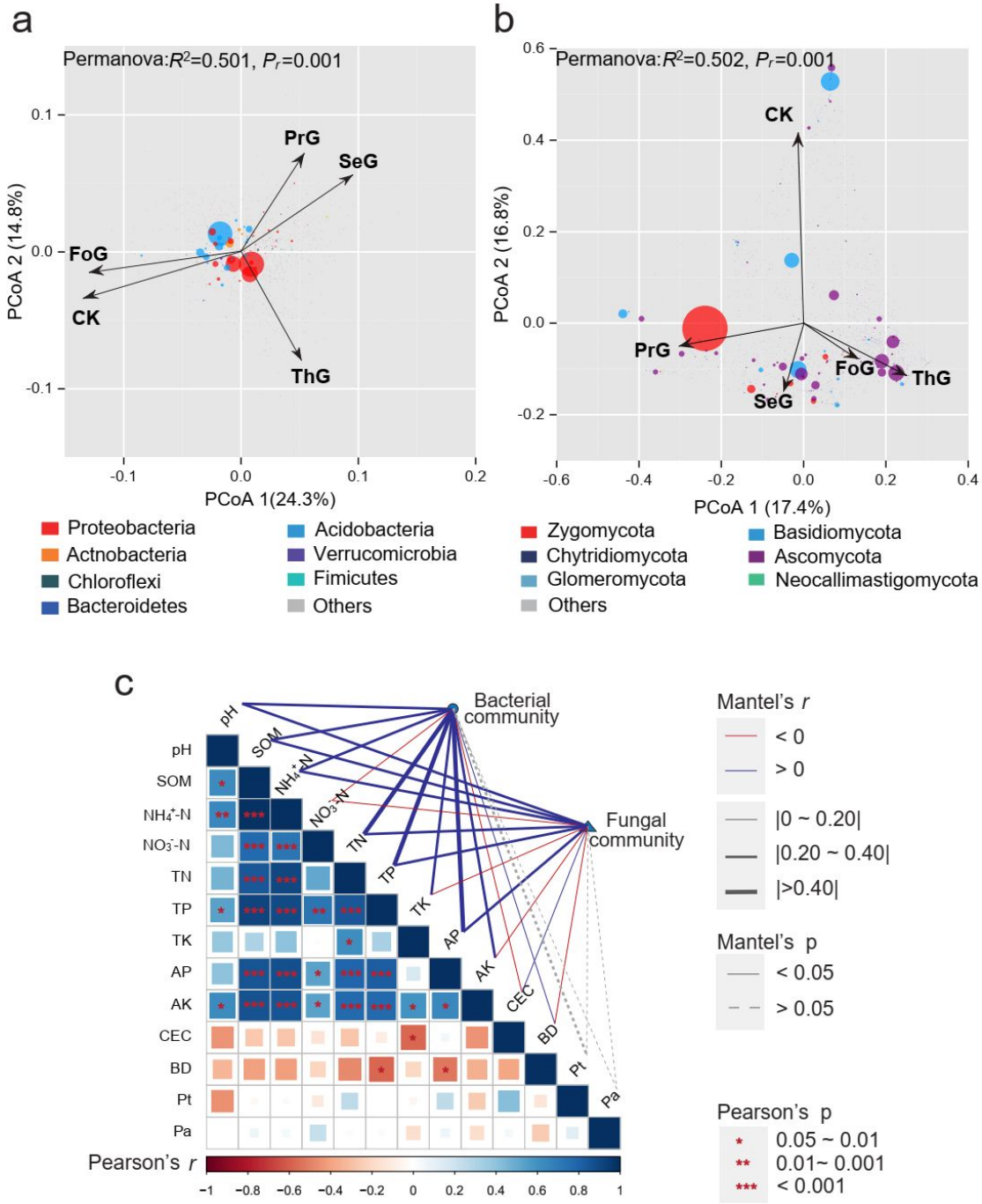

FIGURE S3 Principal coordinate analysis based on the Bray-Curtis distances showing the effects of the *Eucalyptus* plantation on bacterial (a) and fungal (b) communities. The endpoint of the arrow points the central of the treatments. Different colors represent different bacterial and fungal phyla, respectively, and the size of pie represents the average abundance of each phylum. (c) The effects of soil chemical properties on the structure of bacterial and fungal community. PrG, first generation of *Eucalyptus*; SeG, secondary generation of *Eucalyptus*, ThG, third generation of *Eucalyptus*; FoG, fourth generation of *Eucalyptus*; CK, evergreen broadleaf forest as control.

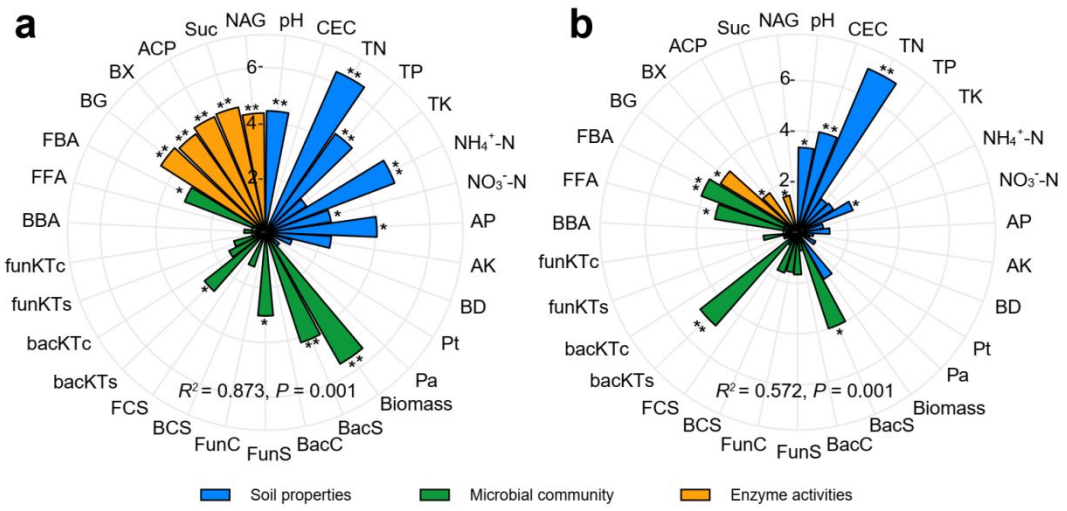

FIGURE S4 Random forest modeling indicates the relative importance of predictors for soil organic carbon (SOC) content (a) and cumulative C mineralization (b). Soil properties include cation exchange capacity (CEC), total nitrogen (TN), total phosphorus (TP), total potassium (TK), ammonium nitrogen (NH_4^+−N), nitrate nitrogen (NO_3^-−N), available phosphorus (AP), available potassium (AK), bulk density (BD), total porosity (Pt), aeration porosity (Pa). Biomass is represented by microbial biomass carbon (MBC), microbial biomass nitrogen (MBN), and microbial biomass phosphorus (MBP). The bacterial and fungal diversity is represented by bacterial and fungal Shannon index (BacS and FunS) and Chao1 richness (BacC and FunC), respectively. The diversity of keystone bacteria and fungi is indicated by Shannon index (BacKTs and FunKTs) and Chao1 richness (BacKTc and FunKTc), respectively. The structure of the bacterial and fungal community (BCS and FCS) is indicated by the first principal coordinate (PCoA1). The bacterial-fungal co-occurrence network is indicated by the proportion of negative to positive bacterial-bacterial (BBA), fungal-fungal (FFA), and fungal-bacterial (FBA) associations, respectively. Soil enzymatic activities include β-1,4-glucosidase (BG), β-xylosidase (BX), acid phosphatase (ACP), sucrase (Sur), and β-N-acetylglucosaminidase (NAG).